Hedgehog: an Attribute to Tumor Regrowth after Chemoradiotherapy and a Target to Improve Radiation Response

Jennifer Sims-Mourtada,[1] Julie G. Izzo,[2] Smith Apisarnthanarax,[1] Tsung-Teh Wu,[3] Usha Malhotra,[2] Rajyalashmi Luthra,[3] Zhongxing Liao,[1] Ritsuko Komaki,[1] Albert van der Kogel,[5] Jaffer Ajani,[4] and K.S. Clifford Chao[1]

Abstract

Purpose: Despite aggressive chemotherapy, radiotherapy, surgery, or combination approaches, the survival rate of patients with esophageal cancer remains poor. Recent studies have suggested that constitutive activation of the Hedgehog (Hh) pathway in cancers of the digestive tract may contribute to the growth and maintenance of cancer. However, the relationship between Hh signaling and therapeutic response is unknown.

Experimental Design: The expression and temporal kinetics of Hh signaling and proliferation biomarkers after chemoradiotherapy were examined in esophageal tumor xenografts. Additionally, immunohistochemical analysis of Sonic Hh (Shh) and Gli-1 expression were done on residual tumors from patients who received neoadjuvant chemoradiotherapy followed by surgery. The ability of Shh signaling to induce proliferation in esophageal cell lines was determined. Expression of cell cycle checkpoint proteins was analyzed in cells in which Hh signaling was activated or inhibited. We further determined the effect of inhibiting Hh signaling in sensitizing esophageal tumors to radiation.

Results: We showed that the Shh signaling pathway was extensively activated in esophageal cancer xenografts and residual tumors after chemoradiotherapy and the temporal kinetics of Hh signaling preceded increases in proliferation biomarker expression and tumor size during tumor regrowth. We further showed that Hh pathway activity influences proliferation rates of esophageal cancer cell lines through up-regulation of the G_1-cyclin-Rb axis. Additionally, we found that blocking Hh signaling enhanced radiation cytotoxicity of esophageal cancer cells.

Conclusions: These results suggest that activation of the Hh pathway may promote tumor repopulation after chemoradiotherapy and contribute to chemoradiation resistance in esophageal cancers.

Cancer of the esophagus is one of the most virulent malignancies, with a 5-year survival rate of <20% (1). The most commonly used therapy for localized esophageal cancer (stages II and III) is chemoradiotherapy followed by surgery (2–5). However, numerous clinical trials have shown that this preoperative strategy benefits only the 25% of patients who have no cancer cells in the resected specimen (pathologic complete response), whereas the remaining 75% present chemoradiotherapy-resistant and highly aggressive cancers (2–5). Nearly all patients experience severe treatment-related morbidities but only a few patients benefit.

An increase in tumor cell proliferation rates after exposure to chemotherapy (6) and radiation (6–8) contributes to tumor resistance and regrowth (6, 7). As the rate of regeneration of tumor cells increases, the effectiveness of each treatment is reduced, implying repopulation by a chemoradiotherapy-resistant clonogenic population in between treatment fractions (6). Previous studies have suggested that unregulated progenitor cell proliferation induced by abnormal activation of the Hh signaling pathway contributes to carcinogenesis of the digestive tract tissues (9, 10). Activation of Hh signaling by binding of secreted Hh ligands (Sonic, Indian, and Desert) to the membrane receptor Patched results in the nuclear translocation and activation of transcription factors of the Gli family (11, 12), whose targets include genes controlling the cell cycle, cell adhesion, signal transduction, angiogenesis, and apoptosis

Authors' Affiliations: Departments of [1]Radiation Oncology, [2]Experimental Therapeutics, [3]Pathology, and [4]Gastrointestinal Medical Oncology, The University of Texas M.D. Anderson Cancer Center, Houston, Texas and [5]Department of Radiation Oncology, Radboud University Nijmegen Medical Center, Nijmegen, The Netherlands

Received 1/25/06; revised 5/2/06; accepted 8/16/06.

Grant support: NIH/National Cancer Institute grants CA89198 and P50 CA121551, Department of Defense grant PC050508, University of Texas M.D. Anderson Multidisciplinary Research Project Grant, Riverkreek Foundation, and the Dallas, Cantu, Smith, and Park Families.

The costs of publication of this article were defrayed in part by the payment of page charges. This article must therefore be hereby marked *advertisement* in accordance with 18 U.S.C. Section 1734 solely to indicate this fact.

Requests for reprints: K.S. Clifford Chao, Department of Radiation Oncology, University of Texas M.D. Anderson Cancer Center, Unit 97, 1515 Holcombe Boulevard, Houston, TX 77030. Phone: 713-563-2300; Fax: 713-563-2331; E-mail: cchao@mdanderson.org.

doi:10.1158/1078-0432.CCR-06-0176

(13). Additionally, Gli-1 is a transcriptional target of the Hh pathway (14), providing positive feedback for Hh signaling. Treatment of cancer cell lines with the Hh-inhibitory compound cyclopamine results in down-regulation of the proliferation marker Ki67 and reduced proliferation rates (9, 15, 16), indicating that Hh pathway activation may be essential for tumor growth and maintenance. However, the significance of Hh signaling in chemoradiotherapy-resistant tumors is not clear. Here, we provide evidence that release of Shh ligand and subsequent activation of the Hh signaling pathway may support tumor repopulation after chemoradiotherapy. Therefore, the Hh pathway is a potential target for improving responses to chemoradiotherapy.

Materials and Methods

Cell lines and antibodies. SEG-1, SKGT4, Bic-1, and BE-3 esophageal adenocarcinoma cells were cultured in DMEM supplemented with 10% fetal bovine serum. Polyclonal antibodies to Gli-1 (H-300), cyclin-dependent kinase 4 (C22), Shh (H-160), and cyclin D1 (HD-11) were obtained from Santa Cruz Biotechnology, Inc. (Santa Cruz, CA). Rb (4H1) and phospho-Rb Ser^{780} were obtained from Cell Signaling Technologies (Danvers, MA). The antibody to Ki67 (B56) was obtained from BD PharMingen (San Diego, CA). 9F1, a rat monoclonal antibody to mouse endothelium, was obtained from the Department of Pathology, Radboud University Nijmegen Medical Center, The Netherlands. The antibody to bromodeoxyuridine was obtained from Abcam Ltd. (Cambridge, MA).

Patient selection and tissue specimens. Cancer specimens were obtained from 43 patients that participated in clinical trials approved by the University of Texas M.D. Anderson Institutional Review Board. Patients with localized (T_1N_1, T_2-T_3 with any N or with M_{1a}) and histologically confirmed adenocarcinoma or squamous cell carcinoma of the thoracic esophagus received preoperative chemoradiation followed by transthoracic or transhiatal esophagectomy that included mediastinal and celiac lymphadenectomy. Tissue specimens in this report were residual esophageal cancer–resected specimens. Each esophageal-resected specimen was examined in a very elaborated manner (17) and was reverified by one experienced gastrointestinal pathologist (T.T.W.) who had no knowledge of patient outcome. The pathologic response was determined in the resected esophagus and was assigned two categories: no residual carcinoma in the esophagus (pathCR), or any residual carcinoma in the resected specimen (<pathCR). Tissue specimens were acquired through an approved protocol by the University of Texas M.D. Anderson Institutional Review Board and after informed consent from patients. All cancer tissues sections were matched with routine H&E-stained slides used to evaluate for the presence of cancer cells by one gastrointestinal specialized pathologist (T.T.W.).

Mouse tumor model. Five-month-old Swiss *nu/nu* mice were obtained from the specific pathogen-free mouse colony of the Department of Experimental Radiation Oncology, M.D. Anderson Cancer Center, Houston, TX. Single SEG-1 tumor xenografts were generated in the right hind limbs of the mice by i.m. injection of 10 μL of a single-cell suspension of 1×10^6 tumor cells. Once the tumors achieved a mean diameter of 8 mm, measured by three orthogonal diameters with Vernier calipers, the mice were randomly partitioned to different treatment groups (described below).

Chemoradiotherapy treatment of xenografts. Sequential chemoradiotherapy was given to the mice as previously described (18). The docetaxel (Sigma Chemical Co., St. Louis, MO) treatment solution was prepared by mixing 1 volume of ethanolic stock solution (50 mg/mL) of docetaxel, 1 volume of polysorbate 80 (Sigma, St. Louis, MO), and 19 volumes of 5% glucose in water. The i.v. injection volume per mouse was 33 mg/kg, or 0.4 mL for a 30-g mouse. This dose of docetaxel is roughly equivalent to the clinically used human dose of 100 mg/m^2. Tumors were locally irradiated 24 hours after docetaxel treatment with a single 15-Gy dose using a small-animal ^{137}Cs irradiator (Nasatron, U.S. Nuclear, Burbank, CA). Radiation was given under ambient-air breathing conditions at a dose rate of 5.4 Gy/min. During irradiation, the unanesthetized mice were mechanically immobilized on a jig, and the tumor was centered in a circular field 3 cm in diameter. Tumor diameters were determined every other day to monitor growth.

Immunofluorescence staining. Pimonidazole [1-((2-hydroxy-3-piperidinyl)propyl)-2-nitroimidazolehydrochloride; Sigma] was used as a marker of hypoxia. Pimonidazole (20 mg/mL) was combined with the perfusion marker Hoechst 33342 (Serva, Heidelberg, Germany; 3.75 mg/mL), and 0.1 mL of this solution was injected i.v. in the tail vein of each mouse. The S-phase marker bromodeoxyuridine (Sigma; 2.5 mg/mL) was injected i.p. at a dose of 0.5 mL. Pimonidazole/Hoechst and bromodeoxyuridine were injected 25 minutes before the animals were killed by cervical dislocation. Tumors were removed immediately, and frozen sections were made and stained as previously described (19).

Immunohistochemistry and protein expression. Immunohistochemical staining for Shh and Gli-1 was done on 4-μm formalin-fixed, paraffin-embedded adjacent sections of SEG-1 tumor xenografts and human residual cancer obtained after esophagectomy. Rabbit polyclonal antibodies Shh (H-160; concentration, 2 μg/mL) and Gli-1 (H-330; concentration, 4 μg/mL) were obtained from Santa Cruz Biotechnology. The immunohistochemical procedure was carried out as previously described (20), with some modifications. After deparaffination and rehydration, antigen retrieval was done in a steamer for 30 minutes at 90°C using an acidic solution (Vector Laboratories, Inc., Burlingame, CA). Primary antibodies were incubated overnight at 4°C. As negative controls for determining the specificity of the immunostaining results, we pretreated with blocking peptide (Shh), omitted the primary antibody (Gli-1), and stained a paraffin-embedded pellet of SEG-1 human esophageal adenocarcinoma, known to express an activated Hh pathway (ref. 9; Fig. 1A and B). As a positive control, we used paraffin-embedded cell pellets of SEG-1 that were placed on the same slide that the human or xenografts tissues (Fig. 1C and D).

For the human tissues, to allow comparison between Shh and Gli-1 on a region-by-region basis, adjacent sections were stained, and then digitized images of the sections were captured with a high-resolution image analysis system (SimplePCI, Compix, Inc., Cranberry Town, PA) controlling a Nikon Optiphot microscope equipped with a motorized stage and a 3 CCD color video camera (Sony DXC-390, Sony, Inc., Tokyo, Japan). The digitized field-by-field montage image representing the whole tissues were then used for assessment of relative proteins expression using the MetaMorph image analysis system (Universal Imaging Corp., Downington, PA) to define and compare tumor regions of interest. Only Shh cytoplasmic and Gli-1 nuclear immunoreactivity in tumor cells were considered for scoring purposes. Staining intensity for Shh was defined as undetectable (0) or detectable (1). Staining intensity for Gli-1 was evaluated on a three-point semiquantitative scale as follows: 0, undetectable; 1, weak to moderate; 2, strong staining. The extent of cancer cells with positive Shh and Gli-1 was expressed as the fraction of labeled cells (i.e., staining levels 1 and 2) in the cancer fields. Esophageal residual tumors with positive tumor Shh staining were then classified, based on the percentage of nuclear Gli-1, into four groups: negative, low expression (1% to <30% tumor cells stained), moderate expression (≥30% to <60% tumor cell stained), and strong expression (≥60% tumor cell stained). These groups were defined based on the quartile distribution of the Gli-1 labeling indices, the median (range) being 0.4 (0.03-0.9). Immunoreactions were independently analyzed by three investigators (J.G.I., T.T.W., and U.M.) unaware of the clinical data. In the discrepant cases, a final opinion was made on consensus by all three investigators.

Proliferation assays. Cell proliferation was measured using 3-(4,5-dimethylthiazol-2-yl)-2,5-diphenyltetrazolium bromide assay. Briefly, 5,000 cells were seeded in 96-well plates and incubated in culture

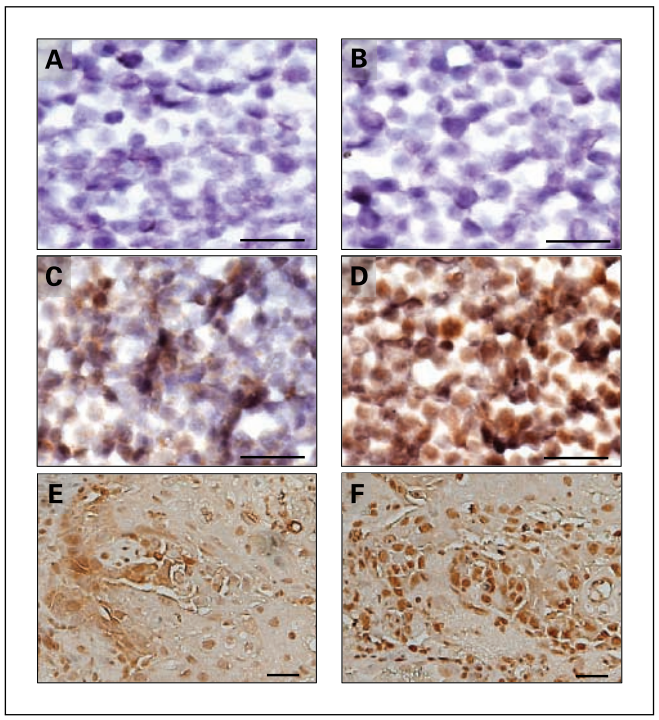

Fig. 1. Activation of Hh pathway is associated with treatment resistance in esophageal adenocarcinoma. *A,* negative control for Shh staining in SEG-1 cells, using Shh-blocking peptide. *B,* negative control (omission of the primary antibody) for Gli1 staining in SEG-1 cell. *C,* Shh cytoplasmic staining in SEG-1 cells. *D,* Gli1 nuclear protein expression in SEG-1 cells. *E* to *F,* immunohistochemical analysis of tissue samples taken from patients with gross residual disease (<pathCR) showing concomitant cytoplasmic Shh staining and nuclear Gli-1. Bar, 50 μm.

medium overnight. Cells were then treated with 200 ng/mL Shh NH_2-terminal peptide (R&D Systems, Minneapolis, MN), 10 μmol/L cyclopamine (LC Labs, Woburn, MA) or transfected with Control or Gli-1 small interfering RNA (siRNA) for 48 hours. At the end of the treatment exposure time, 10 μL of 3-(4,5-dimethylthiazol-2-yl)-2,5-diphenyltetrazolium bromide (Sigma) at a concentration of 10 mg/mL in PBS was added, and the cells were incubated for a further 4 hours at 37°C. Subsequently, 100 μL of DMSO (Sigma) was added, and the plate was incubated for 5 minutes at 37°C to dissolve the formazan crystals. The absorbance was measured at a wavelength of 570 nm on a microplate reader (BioTek, Winooski, VT). Each experiment was repeated at least thrice in triplicate. Results represented the absorbance ratio between the treated and untreated cells at indicated time points. For DNA synthesis studies, cells were treated with 200 ng/mL Shh NH_2-terminal peptide (R&D Systems) for 48 hours or transiently transfected with pCDNA3.1-Gli-1 (21), using Fugene transfection reagent (Roche Applied Biosciences, Indianapolis, IN), according to the manufacturer's instructions 48 hours before the addition of media containing 1 μCi of ^{3}H-thymidine (Sigma-Aldrich, St. Louis, MO). Cells were incubated for an additional 24 hours and then lysed with 10 mol/L NaOH. Radioactivity of cell lysates was measured using a liquid scintillation counter (Tri-Carb 2100TR, Packard, Meridian, CT). Cells treated with PBS or cells transfected with pCNA3.1 vector served as controls. Experiments were done thrice in triplicate.

Immunoblot analysis. SEG-1 cells were plated at 50% confluency in 100-cm plates and grown overnight. Cells were treated with 100 ng/mL recombinant Shh NH_2-terminal peptide for 24 hours before lysis or with 10 μmol/L forskolin, 10 μmol/L cyclopamine, or 100 nmol/L siRNA for 48 hours before lysis. Cells were lysed with radioimmunoprecipitation assay buffer, and protein concentrations were determined using the Bradford assay (Bio-Rad, Hercules, CA). Western blot analysis, using 75 μg of protein, was done as previously described (22).

RNA interference. Double-stranded, purified siRNAs were purchased from Ambion (Austin, TX). The sequences for the Gli-1 and control siRNAs were AACUCCACAGGCAUACAGGAU and AACGUACGCGGAAUACAACGA, respectively. The siRNAs were transfected into cells at 100 nmol/L using Lipofectin (Invitrogen, San Diego, CA) according to the manufacturer's instructions.

Cell cycle analysis. Cells were collected by trypsinization 48 hours after exposure to 10 μmol/L forskolin, 10 μmol/L cyclopamine, or 100 nmol/L siRNA or 24 hours after exposure to radiation (4 Gy). The cells were fixed with 100% ethanol, stained with 10 μg/mL propidium iodide and 5 μg/mL RNase A, and analyzed for fluorescence using a FACScan flow cytometer (Becton Dickinson, San Diego, CA). The proportion of cells in sub-G_0, G_1, S, and G_2-M phases were determined by ModFit software (Verity Software House, Topsham, ME).

Clonogenic survival. Survival after radiation exposure was defined as the ability of cells to maintain clonogenic capacity and form colonies. Briefly, 1×10^6 cells were plated and grown overnight. Cells were treated with 10 μmol/L cyclopamine or 10 μmol/L forskolin and allowed to grow for 24 hours. The cells were then exposed to increasing doses of ionizing radiation plated in 100-mm dishes at varying densities in the presence of the above inhibitors and allowed to grow for 10 days and then stained with crystal violet. Individual colonies were counted, and survival curves were obtained.

Cell viability and caspase-3 activity. Cells were transfected with Gli-1 or Random control siRNA and cultured for 24 hours. Cells were then exposed to 6 Gy ionizing radiation and seeded into 96-well plates. Cell viability was determined 48 hours later by 3-(4,5-dimethylthiazol-2-yl)-2,5-diphenyltetrazolium bromide assay, as described above. Caspase-3 activity was determined using a caspase-3 colorimetric assay kit (R&D Systems) according to the manufacturer's protocol. Briefly, 1×10^6 cells were treated with 10 μmol/L cyclopamine, 10 μmol/L forskolin, or 100 nmol/L siRNA and allowed to grow for 24 hours. The cells were then exposed to ionizing radiation (6 Gy), incubated for an additional 24 hours, trypsinized, and collected by centrifugation, and cell lysates were obtained. Lysates (150-250 μg of protein) were assayed for caspase activity. The specific peptide substrate used was DEAD-*p*NA. Release of the *p*NA cleavage product was quantified in a microplate reader (BioTek) at a wavelength of 405 nm. Each assay was done in triplicate and repeated thrice.

Statistical analysis. For *in vitro* studies, significance was determined by unpaired Student's *t* test. $P < 0.05$ using a two-tailed test was taken as significant for all statistical tests. Computations were carried out using a SAS software package (version 6.12; SAS Institute, Inc., Cary, NC).

Results

To determine if activation of the Hh signaling pathway is associated with therapeutic resistance to chemoradiotherapy, we examined expression levels of Shh and nuclear Gli-1 proteins in esophageal cancer specimens obtained after esophagectomy of 43 patients who received preoperative chemoradiotherapy. All patients that were resistant to chemoradiotherapy (i.e., achieved <pathCR) had residual cancer in the resected specimen. Of the 43 chemoradiotherapy-resistant cancers, 36 (83.7%) had activated Hh signaling (i.e., defined by concomitant cytoplasmic Shh and nuclear Gli-1 expression); 2 (4.6%) had Shh expression without Gli-1 nuclear localization; and 5 (11.7%) were negative for both Shh and Gli-1 expression (Table 1). The median labeling indices for Shh and Gli-1 were 0.08 (range = 0.01-0.8) and 0.4 (range = 0.03-0.9), respectively. Among cancers with activated Hh, 9 had low, 15 had moderate, and 12 had strong Gli-1 nuclear expression (Table 1). Gli-1 nuclear expression was never observed without concomitant Shh expression. Figure 1 shows examples of Shh and Gli-1

Table 1. Shh and Gli1 protein expressions in 43 human esophageal cancers resistant to chemoradiation

	Total (43)	Gli1 expression*			
		Negative	Low	Moderate	Strong
Shh† (+)	38	2 (4.6)	9 (21.0)	15 (34.8)	12 (27.9)
Shh (−)	5	5 (11.7)	0 (0.0)	0 (0.0)	0 (0.0)

*Gli1 nuclear staining in tumor cells is defined as negative (0% stained cells), low (1% to <30% stained cells), moderate (≥30 to <60% stained cells), and strong (≥60% stained cells).
†Shh cytoplasmic immunolocalization in tumor cells.

immunochemical detection. Of interest, when analyzing the spatial localization of Shh and Gli-1 immunostaining within a tumor, Shh staining was usually clustered in small patches surrounded by larger areas of Gli-1 nuclear expression, suggesting a regional activation of the Hh signaling pathway. The substantial expression of Shh in patients with residual cancer after chemoradiotherapy suggests that the secretion of Shh and subsequent activation of the Hh signaling pathway support the proliferation and survival of cancer cells after treatment.

To address the role of the Shh/Gli-1 signaling pathway in persistent disease or subsequent regrowth of tumor after chemoradiotherapy, we used an esophageal adenocarcinoma tumor xenograft model. A xenograft model was chosen due to the lack of a suitable murine orthotopic model of esophageal cancer. SEG-1 esophageal adenocarcinoma xenografts were generated by i.m. injection of tumor cells into the hind limbs of nude mice. The resulting tumors were treated with docetaxel (33 mg/kg i.v.) and 15 Gy of ionizing radiation. This *in vivo* chemoradiotherapy model temporarily delays the growth of tumors but is not sufficient to eradicate the tumor, a scenario that is observed in the clinical setting for treatment-resistant tumors. As shown in Fig. 2A, baseline untreated tumors exhibited chronic hypoxia and a high rate of proliferation occurring close to vessels. However, 2 days after treatment, proliferation rates were strongly reduced. Some proliferating cells were observed, but these were located farther away from vessels. By 6 to 8 days after chemoradiotherapy, tumor repopulation had begun, and small islands of proliferating cells were observed in the stroma. On day 10, high rates of proliferation were observed. In contrast to the diffuse proliferation observed close to vessels at earlier time points, foci of proliferating colonies were evident.

To determine the relationship between Hh expression and proliferation after chemoradiotherapy, we examined temporal changes in expression of Shh ligand or Gli-1 nuclear translocation along with changes in the proliferation biomarker Ki67 and tumor size before and after chemoradiotherapy. As shown in Fig. 2B, a partial treatment response was observed, characterized by an initial decrease in tumor size 4 to 6 days after treatment and subsequent tumor regrowth after day 10. A decrease in Ki67 staining was seen as early as 4 hours after chemoradiotherapy. Proliferation rates continued to decline until 4 days after treatment and increased substantially 8 days after chemoradiotherapy preceding an increase in tumor size. Low-level expression of cytoplasmic Shh and nuclear Gli-1 (i.e., weak to moderate staining intensity and lower labeling index) was observed before chemoradiotherapy. Similar to the expression patterns observed in the resected cancer specimens, Shh expressing cells were spatially localized in small clusters throughout the tumor, whereas Gli-1 expressing cells seemed more diffusely distributed in the vicinity of Shh-positive clusters. However, 6 to 8 days after chemoradiotherapy, and just before the increase in tumor proliferation rates, we observed a substantial increase in Hh activity, characterized by (*a*) increased number of clustered cells expressing strong cytoplasmic Shh, (*b*) distinct Shh staining in the intercellular spaces surrounding the clusters, and (*c*) significant increase in nuclear Gli-1 labeling indices patching the tumor fields. These observations depict the temporal kinetics of SHH ligand release and Gli-1 activation before repopulation of surviving tumor cells after chemoradiotherapy.

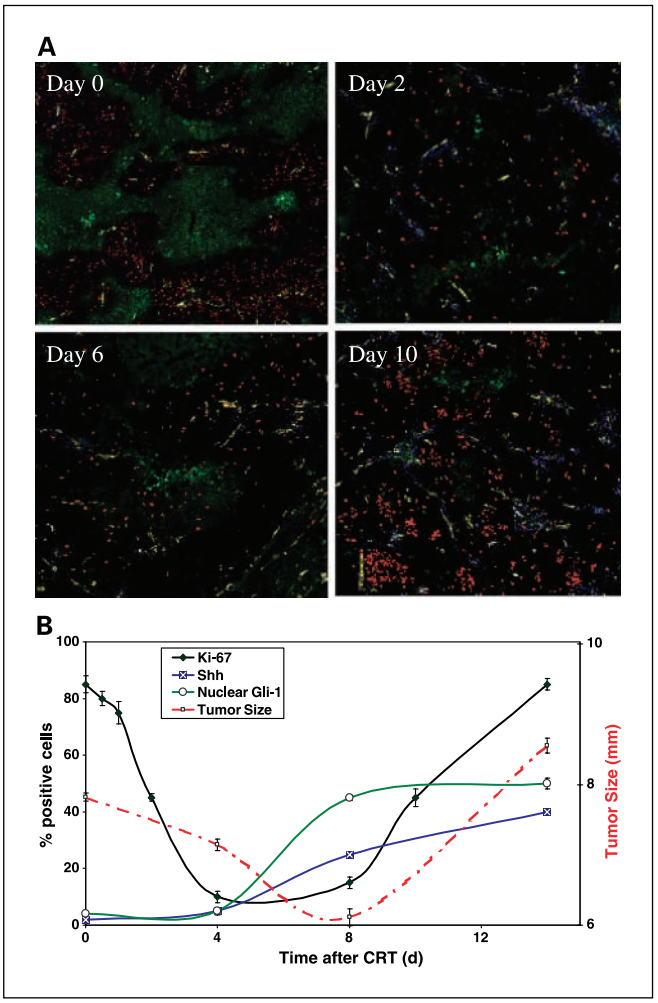

Fig. 2. Temporal kinetics of Hh pathway activation precedes tumor cell proliferation and regrowth after chemoradiotherapy in esophageal adenocarcinoma xenografts. *A*, multiparameter analysis of SEG-1 tumor sections at 0, 2, 6, and 10 days after chemoradiotherapy. Green, hypoxia; red, proliferation; blue, perfusion; white, vessels. Proliferation of clonogenic foci is apparent 10 days after treatment. *B*, results of immunohistochemical analysis showing increase of Shh and nuclear Gli-1 expression precedes increases in Ki67 staining (*left axis*) and tumor size (*right axis*) during tumor repopulation after chemoradiotherapy. Points, mean of three independent experiments; bars, SD.

To determine the causative relationship between Hh signaling and proliferation of esophageal tumor cells, three esophageal adenocarcinoma cell lines (SKGT4, SEG-1, and Bic1) were treated with exogenous Shh ligand, the Hh pathway antagonist cyclopamine, which blocks SMO receptor activation, or a Gli-1-specific siRNA. Activation or inhibition of Hh signaling was confirmed by detecting Gli-1 nuclear translocation using immunofluorescence-based confocal microscopy (Fig. 3A). Additionally, because Gli-1 is a transcriptional target of the Hh pathway (14), inhibition of Hh signaling was confirmed by a decrease in Gli-1 expression in cells treated with Hh inhibitors or Gli-1-specific siRNA compared with controls (Fig. 3B). After 48 hours of treatment with cyclopamine or Gli-1 siRNA, a significant decrease in proliferation was observed (Fig. 3C), whereas a significant increase in proliferation rates was observed in cells treated with exogenous Shh ligand. The degree of response correlated with level of endogenous Gli-1 expression (Fig. 3D), indicating that this effect is specific to Hh signaling. To further explore the relationship between Hh activation and proliferation of esophageal cancer, DNA synthesis levels of cells stimulated with Shh ligand were measured by ^{3}H-thymidine incorporation and compared with baseline levels obtained with vehicle-treated control cells. A significant increase in ^{3}H-thymidine incorporation was observed in Shh treated cells compared with untreated controls.

Similar results were obtained with cells transiently overexpressing nuclear Gli-1 (Fig. 3E). These results show that Hh signaling can promote a significant proliferative response in esophageal tumor cells.

Dysregulation of cell cycle regulatory proteins contributes to the proliferation of tumor cells and subsequent repopulation of tumors after chemoradiotherapy (23). To determine the mechanism of Shhinduced proliferation, we analyzed the expression levels of cyclin D1 in SEG-1 cells upon exogenous stimulation of Hh signaling. As shown in Fig. 4A, there is an increase in cyclin D1 protein expression in Shh stimulated cells compared with controls. We also examined the levels of Rb expression and activation in Shh-treated cells. Although there was no significant change in Rb protein levels, a significant increase in Rb phosphorylation at the cyclin D phosphorylation site (Ser^{780}) was observed. These results indicate that Shh stimulation in esophageal tumor cells can promote G_1-S cell cycle phase transition by increasing activity of the cyclin-Rb axis.

To examine the effect of Hh signaling on the cell cycle distribution of esophageal adenocarcinoma, SEG-1 cells were treated with the Hh pathway antagonists cyclopamine (which

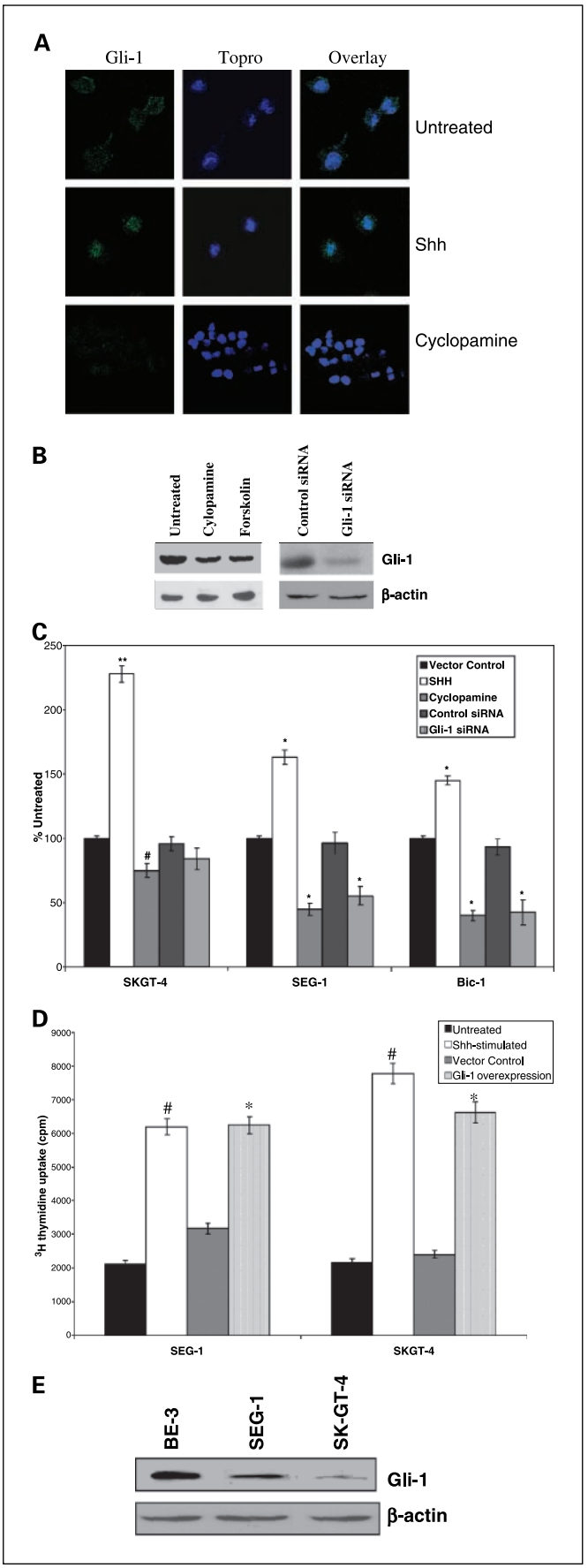

Fig. 3. Activation of Hh signaling induces proliferation of esophageal tumor cells. *A,* immunofluorescence analysis showing an increase in expression and Gli-1 nuclear of SEG-1 cells treated with Shh ligand and a decrease in expression and nuclear translocation of Gli-in cells treated with cyclopamine. *B,* Western blot analysis showing decrease in expression of the Hh target Gli-1 in cells treated with Hh signaling inhibitors cyclopamine and forskolin, or transfected with Gli-1 siRNA. *C,* 3-(4,5-dimethylthiazol-2-yl)-2,5-diphenyltetrazolium bromide analysis showing increased proliferation of cells treated with exogenous Shh ligand compared with untreated controls and reduced proliferation rates in cells treated with the Hh inhibitor cyclopamine or Gli-1 siRNA compared with vector controls. #, $P < 0.05$; *, $P < 0.01$; **, $P < 0.001$. *D,* Western analysis showing differential Gli-1 protein expression in Bic-1, SEG-1, and SKGT-4 esophageal adenocarcinoma cell lines. *E,* increase in ^{3}H-thymidine uptake in SEG-1 cells treated with exogenous Shh ligand (#, $P < 0.01$) or transiently overexpressing Gli-1 (*, $P < 0.05$) compared with controls. Columns, mean of three independent experiments; bars, SD.

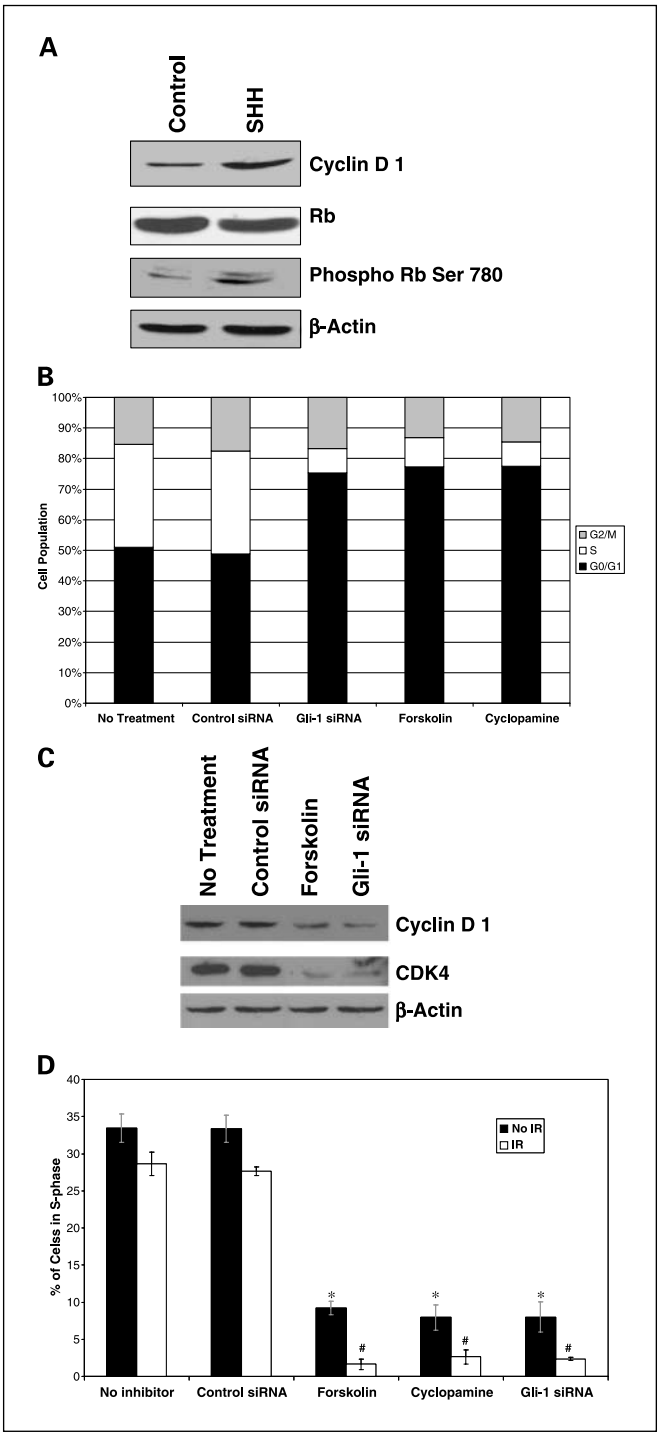

Fig. 4. Inhibition of Hh signaling results in G_1 arrest and decreases percentage of radioresistant S-phase cells in combination with ionizing radiation (*IR*). *A,* Western blot analysis showing up-regulation of cyclin D1 and Rb phosphorylation at Ser^{780} in cells treated with exogenous Shh ligand. *B,* increase in percentage of cells in G_1 phase of cell cycle in cells treated with inhibitors to the Hh pathway compared with untreated controls. Percentages of SEG-1 cells, with or without treatment with Hh inhibitors, in each cell cycle phase. Representative of the means of three separate experiments. *C,* Western blot showing down-regulation of the G1 checkpoint proteins cyclin D1 and cyclin-dependent kinase 4 (*CDK4*) after treatment with Hh inhibitors compared with levels in untreated cells. Actin is shown as a loading control. *D,* percentage of S-phase cells decreases in cells treated with Hh inhibitors combined with ionizing radiation compared with untreated controls. Percentage of S-phase cells with or without exposure to 4 Gy of ionizing radiation. *, $P < 0.01$ for combination of Hh inhibitors and ionizing radiation compared with Hh inhibitors alone. #, $P < 0.005$ for combined treatment compared with untreated controls.

blocks receptor activation), forskolin (which inhibits Gli-1 transcriptional activity; ref. 24), or Gli1 siRNA. Inhibition of Hh signaling was confirmed by analysis of Gli-1 protein expression (data not shown). Consistent with previous reports (15, 25), blocking Hh signaling inhibited cell cycle progression, resulting in the accumulation of cells in the G_1 phase of the cell cycle (Fig. 4B), as a result of decreased expression of the G_1-S checkpoint proteins cyclin D1 and cyclin-dependent kinase 4 (Fig. 4C).

It is well established that the sensitivity of cells to the cytotoxic effects of radiation is cell cycle dependent, with the S phase being more resistant and the G_1-S boundary and G_2-M phase being more sensitive (26). Treatment of SEG-1 cells with ionizing radiation alone led to a slight but not significant reduction in the radiation-resistant S-phase fraction (Fig. 4D). Treatment with Hh inhibitors alone led to a significant ($P < 0.01$) reduction in the S-phase fraction, and the combination of radiation and Hh inhibitors caused a greater reduction ($P < 0.005$) in the S-phase fraction compared with untreated cells. To determine whether inhibition of Hh signaling can sensitize cells to the cytotoxic effects of radiation, SEG-1 or BE-3 cells were treated with Hh pathway inhibitors in combination with increasing doses of ionizing radiation, and clonogenic survival curves were generated. Inhibition of Hh signaling synergistically decreased the clonogenic survival of tumor cells when combined with radiation (Fig. 5A). Blocking Hh signaling also significantly reduced the shoulder region of the ionizing radiation survival curve, indicating that repair of the sublethal damage induced by ionizing radiation was inhibited. We further evaluated whether the synergistic effect of combining Hh inhibition and radiation involves apoptosis. Although treatment with ionizing radiation alone had little effect on cell viability 48 hours after treatment of esophageal adenocarcinoma cell lines (SEG-1, Bic-1, BE-3, and SK5), a significant decrease in cell viability was observed in cells in which Hh signaling was inhibited (Fig. 5B). Cell viability was further reduced by combination of ionizing radiation and Hh inhibition. Minimal apoptosis, as determined by caspase-3 activity, was observed in esophageal adenocarcinoma cell lines treated with ionizing radiation alone (Fig. 5C and D). Treatment with Hh inhibitors alone induced significant apoptosis, and combined treatment with ionizing radiation and Hh inhibitors resulted in a significantly greater amount of apoptosis.

Discussion

The Hh pathway is critical for tissue growth and differentiation during embryonic development of the gastrointestinal tract tissues (27). In adult cells, Hh signaling has been implicated in the maintenance of homeostasis of stem or progenitor cells in a number of epithelial tissues, including intestinal epithelia (28–30). Additionally, Hh signaling contributes to physiologic processes of epithelial repair and regeneration after injury (29). In normal tissues, Hh-induced progenitor cell proliferation is transient and tightly regulated, preventing continuous regeneration. However, aberrant activation of Hh signaling in tumors may allow escape from regulatory mechanisms that cause the return to quiescence that normally follows regeneration. The activation of the Hh signaling pathway observed in both chemoradiotherapy-resistant

residual esophageal carcinoma specimens (Fig. 1) and animal tumor xenografts (Fig. 2B) suggests that release of Shh ligands may support proliferation and survival of tumor clonogens after chemoradiotherapy in an autocrine-paracrine manner. The observation of the differential labeling indices between Shh and Gli-1, and the organization of Gli-1 staining usually surrounding Shh-expressing cell clusters, underscore our hypothesis. Secretion of Shh ligand by tumor cells could have a double effect, by directly stimulating proliferation of surrounding cancer cells and also by promoting release of growth factors necessary for tumor maintenance, such as vascular endothelial growth factor and epidermal growth factor, from stromal cells.

Our data show that stimulation of esophageal cancer cells with Shh ligand or Gli-1 overexpression results in up-regulation of G_1-cyclin activity and increased proliferation. These data suggest that unregulated Hh signaling within tumors may promote a continuous state of tissue repair and clonogenic proliferation once the tumor volume is reduced after chemoradiotherapy, contributing to tumor repopulation. Although a role for Hh signaling has been established in the formation and maintenance of a number of tumors, including basal cell, prostate, breast, and pancreatic carcinomas among others (9, 10, 29, 31–33), our study is the first to examine Hh activation in the context of tumor repopulation after chemoradiotherapy and suggests that in addition to its reported roles in carcinogenesis and tumor maintenance, aberrant activation of the Hh pathway may contribute to tumor repopulation and treatment failure.

Esophageal adenocarcinoma is presently the cancer with the greatest increase in incidence in the United States (34, 35). Currently available treatments of localized cancer of the esophagus are ineffective in >75% of esophageal cancers (chemoradiotherapy resistant), resulting in a 5-year survival rate under 25%. Patients with esophageal cancer and treating oncologists face serious challenge of not being able to optimize therapy. Therapies are currently chosen empirically without concern for tumor and patient heterogeneity. Highly morbid surgery could be avoided if one could identify a molecular signature that would suggest a highly chemoradiation-sensitive cancer. Similarly, understanding the mechanisms resulting in chemotherapy or radiotherapy resistance would allow identification of exploitable targets. The discovery that inhibition of Hh activity can sensitize tumor cells to the effects of radiation suggests that incorporating targeted inhibition of the Hh signaling pathway into current chemoradiotherapy regimens might improve treatment outcome.

There are presently no clinically approved systemic inhibitors of Hh signaling. Topical application of cyclopamine has been

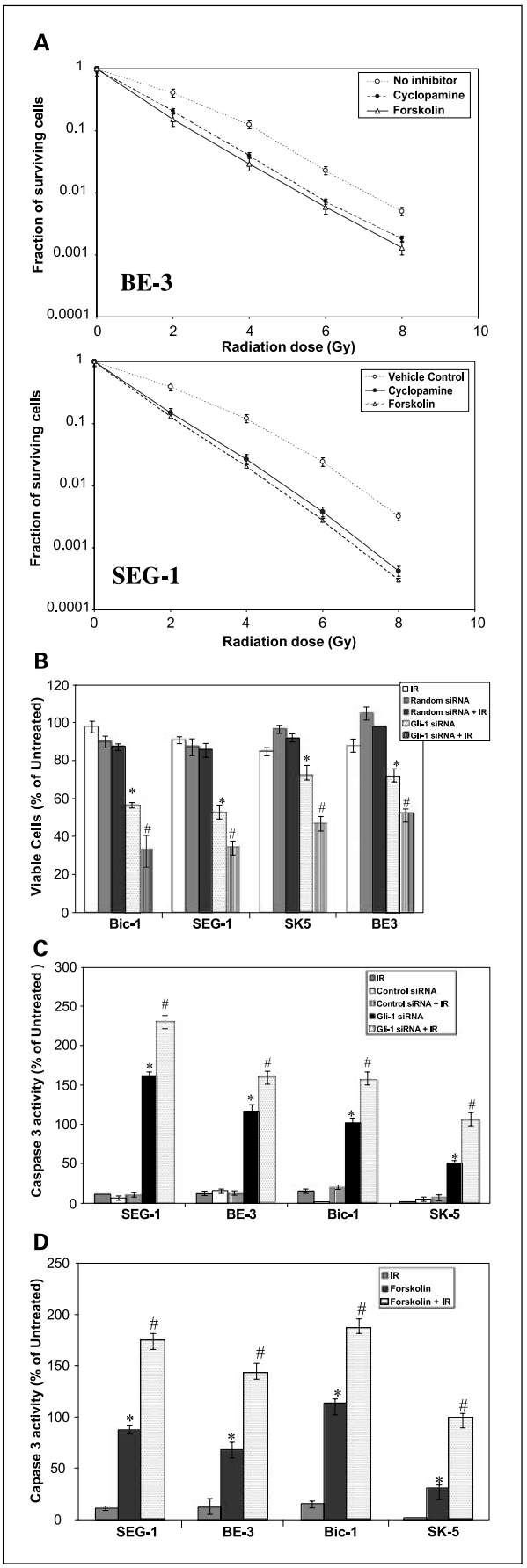

Fig. 5. Radiosensitization of tumor cells by inhibition of Hh signaling. *A,* clonogenic survival curves showing decreased survival of cells treated with Hh inhibitors in combination with ionizing radiation (dose range = 2-8 Gy) compared with irradiated controls in SEG-1 and BE3 cell lines. Survival decreases with increasing dose. *B,* cell viability following treatment with ionizing radiation and/or Gli-1 siRNA or a random control siRNA as determined by 3-(4,5-dimethylthiazol-2-yl)-2,5-diphenyltetrazolium bromide assay. Treatment with Gli-1 siRNA significantly decreased cell viability in all cell lines (*, $P < 0.01$) compared with untreated controls. Combination treatment with ionizing radiation and Gli-1 siRNA resulted in a further significant reduction in cell viability (#, $P < 0.005$). *C,* caspase-3 activity is increased in esophageal adenocarcinoma cell lines treated with ionizing radiation and/or forskolin or (*D*) Gli-1 siRNA compared with untreated cells and cells treated with ionizing radiation alone. Percentage of caspase-3 activity in untreated control cells. *, $P < 0.05$; #, $P < 0.005$, compared with untreated control cells.

shown to inhibit the growth of human basal cell carcinoma (36); however, concerns of neurologic disturbances may limit the systemic application of this drug. Several small molecule compounds that prevent Hh signaling by binding to and inhibiting Smo are currently under development, including Cur61414 (37), which has shown promising results in inhibition of basal cell carcinoma and pancreatic cancer in preclinical models. The therapeutic effects of Hh pathway blockade in combination with current chemoradiotherapy regimens are yet to be investigated. Particularly, the differential regulation and timing of Hh activity in normal and tumor tissue after chemoradiotherapy should be further investigated to determine the most beneficial therapeutic index (i.e., effects on normal tissue repair versus tumor).

Acknowledgments

We thank Dr. Mien-Chie Hung for the use of the Olympus Confocal Microscopy Image Analysis System and Dr. Rakesh Kumar for the use of the Olympus DP Controller Image analysis System.

References

1. Parkin DM, Bray F, Ferlay J, et al. Global cancer statistics, 2002. CA Cancer J Clin 2005;55:74–108.
2. Coia LR, Minsky BD, Berkey BA, et al. Outcome of patients receiving radiation for cancer of the esophagus: results of the 1992–1994 Patterns of Care Study. J Clin Oncol 2000;18:455–62.
3. Brenner B, Ilson DH, Minsky BD. Treatment of localized esophageal cancer. Semin Oncol 2004;31:554–65.
4. Iyer R, Wilkinson N, Demmy T, et al. Controversies in the multimodality management of locally advanced esophageal cancer: evidence-based review of surgery alone and combined-modality therapy. Ann Surg Oncol 2004;11:665–73.
5. Urba S. Esophageal cancer: preoperative or definitive chemoradiation. Ann Oncol 2004;15:93–6.
6. Tannock IF. Tumor physiology and drug resistance. Cancer Metastasis Rev 2001;20:123–32.
7. Milas L, Yamada S, Hunter N, et al. Changes in TCD_{50} as a measure of clonogen doubling time in irradiated and unirradiated tumors. Int J Radiat Oncol Biol Phys 1991;21:1195–202.
8. Fowler JF, Lindstrom MJ. Loss of local control with prolongation in radiotherapy. Int J Radiat Oncol Biol Phys 1992;23:457–67.
9. Berman DM, Karhadkar SS, Maitra A, et al. Widespread requirement for Hedgehog ligand stimulation in growth of digestive tract tumours. Nature 2003;425:846–51.
10. Watkins DN, Peacock CD. Hedgehog signalling in foregut malignancy. Biochem Pharmacol 2004;68:1055–60.
11. Ingham PW, McMahon AP. Hedgehog signaling in animal development: paradigms and principles. Genes Dev 2001;15:3059–87.
12. Ruel L, Rodriguez R, Gallet A, et al. Stability and association of Smoothened, Costal2 and Fused with *Cubitus interruptus* are regulated by Hedgehog. Nat Cell Biol 2003;5:907–13.
13. Yoon JW, Kita Y, Frank DJ, et al. Gene expression profiling leads to identification of GLI1-binding elements in target genes and a role for multiple downstream pathways in GLI1-induced cell transformation. J Biol Chem 2002;277:5548–55.
14. Dai S, Huang ML, Hsu CY, et al. Inhibition of hypoxia inducible factor 1α causes oxygen-independent cytotoxicity and induces p53 independent apoptosis in glioblastoma cells. Int J Radiat Oncol Biol Phys 2003;55:1027–36.
15. Karhadkar SS, Bova GS, Abdallah N, et al. Hedgehog signalling in prostate regeneration, neoplasia and metastasis. Nature 2004;431:707–12.
16. Ma X, Sheng T, Zhang Y, et al. Hedgehog signaling is activated in subsets of esophageal cancers. Int J Cancer 2005;118:139–48.
17. Chirieac LR, Swisher SG, Ajani JA, et al. Posttherapy pathologic stage predicts survival in patients with esophageal carcinoma receiving preoperative chemoradiation. Cancer 2005;103:1347–55.
18. Mason KA, Hunter NR, Milas M, et al. Docetaxel enhances tumor radioresponse *in vivo*. Clin Cancer Res 1997;3:2431–8.
19. van Laarhoven HW, Bussink J, Lok J, et al. Modulation of hypoxia in murine liver metastases of colon carcinoma by nicotinamide and carbogen. Radiat Res 2005;164:245–9.
20. Izzo JG, Papadimitrakopoulou VA, Liu DD, et al. Cyclin D1 genotype, response to biochemoprevention, and progression rate to upper aerodigestive tract cancer. J Natl Cancer Inst 2003;95:198–205.
21. Bigelow RL, Chari NS, Unden AB, et al. Transcriptional regulation of bcl-2 mediated by the sonic hedgehog signaling pathway through gli-1. J Biol Chem 2004;279:1197–205.
22. Sims-Mourtada JC, Bruce S, McKeller MR, et al. The human AKNA gene expresses multiple transcripts and protein isoforms as a result of alternative promoter usage, splicing, and polyadenylation. DNA Cell Biol 2005;24:325–38.
23. Xia F, Powell SN. The molecular basis of radiosensitivity and chemosensitivity in the treatment of breast cancer. Semin Radiat Oncol 2002;12:296–304.
24. Kaesler S, Luscher B, Ruther U. Transcriptional activity of GLI1 is negatively regulated by protein kinase A. Biol Chem 2000;381:545–51.
25. Fan L, Pepicelli CV, Dibble CC, et al. Hedgehog signaling promotes prostate xenograft tumor growth. Endocrinology 2004;145:3961–70.
26. Hall E. Radiobiology for the radiologist. 5th ed. Philadelphia: Lippincott Williams & Wilkins; 2000.
27. Harmon EB, Ko AH, Kim SK. Hedgehog signaling in gastrointestinal development and disease. Curr Mol Med 2002;2:67–82.
28. Adolphe C, Narang M, Ellis T, et al. An *in vivo* comparative study of sonic, desert and Indian hedgehog reveals that hedgehog pathway activity regulates epidermal stem cell homeostasis. Development 2004;131:5009–19.
29. Beachy PA, Karhadkar SS, Berman DM. Tissue repair and stem cell renewal in carcinogenesis. Nature 2004;432:324–31.
30. Nielsen CM, Williams J, van den Brink GR, et al. Hh pathway expression in human gut tissues and in inflammatory gut diseases. Lab Invest 2004;84:1631–42.
31. Katano M. Hedgehog signaling pathway as a therapeutic target in breast cancer. Cancer Lett 2005;227:99–104.
32. Olsen CL, Hsu PP, Glienke J, et al. Hedgehog-interacting protein is highly expressed in endothelial cells but down-regulated during angiogenesis and in several human tumors. BMC Cancer 2004;4:43.
33. Williams JA. Hedgehog signaling pathway as a target for therapeutic intervention in basal cell carcinoma. Drug News Perspect 2003;16:657–62.
34. Kubo M, Nakamura M, Tasaki A, et al. Hedgehog signaling pathway is a new therapeutic target for patients with breast cancer. Cancer Res 2004;64:6071–4.
35. DeMeester SR. Adenocarcinoma of the esophagus and cardia: a review of the disease and its treatment. Ann Surg Oncol 2006;13:12–30.
36. Tas S, Avci O. Rapid clearance of psoriatic skin lesions induced by topical cyclopamine. A preliminary proof of concept study. Dermatology 2004;209:126–31.
37. Williams JA, Guicherit OM, Zaharian BI, et al. Identification of a small molecule inhibitor of the hedgehog signaling pathway: effects on basal cell carcinoma-like lesions. Proc Natl Acad Sci U S A 2003;100:4616–21.

Clinical Cancer Research

Hedgehog: an Attribute to Tumor Regrowth after Chemoradiotherapy and a Target to Improve Radiation Response

Jennifer Sims-Mourtada, Julie G. Izzo, Smith Apisarnthanarax, et al.

Clin Cancer Res 2006;12:6565-6572.